

Extracting an entangled photon pair from collectively decohered pairs at a telecommunication wavelength

Yoshiaki Tsujimoto,^{1,*} Yukihiro Sugiura,¹ Makoto Ando,¹
Daisuke Katsuse,¹ Rikizo Ikuta,¹ Takashi Yamamoto,¹
Masato Koashi,² and Nobuyuki Imoto¹

¹Graduate School of Engineering Science, Osaka University, Toyonaka, Osaka 560-8531, Japan

²Photon Science Center, The University of Tokyo, Bunkyo-ku, Tokyo 113-8656, Japan

*tsujimoto@mp.es.osaka-u.ac.jp

Abstract: We experimentally demonstrated entanglement extraction scheme by using photons at the telecommunication band for optical-fiber-based quantum communications. We generated two pairs of non-degenerate polarization entangled photons at 780 nm and 1551 nm by spontaneous parametric down-conversion and distributed the two photons at 1551 nm through a collective phase damping channel which gives the same amount of random phase shift on the two photons. Through local operation and classical communication, we extracted an entangled photon pair from two phase-disturbed photon pairs. An observed fidelity of the extracted photon pair to a maximally entangled photon pair was 0.73 ± 0.07 which clearly shows the recovery of entanglement.

© 2018 Optical Society of America

OCIS codes: (270.5565) Quantum communications; (270.5585) Quantum information and processing; (270.0270) Quantum optics; (060.0060) Fiber optics and optical communications; (060.5565) Quantum communications.

References and links

1. C. H. Bennett, G. Brassard, C. Crépeau, R. Jozsa, A. Peres, and W. K. Wootters, “Teleporting an unknown quantum state via dual classical and einstein-podolsky-rosen channels,” *Phys. Rev. Lett.* **70**, 1895–1899 (1993).
2. C. H. Bennett and S. J. Wiesner, “Communication via one- and two-particle operators on einstein-podolsky-rosen states,” *Phys. Rev. Lett.* **69**, 2881–2884 (1992).
3. C. H. Bennett, G. Brassard, and N. D. Mermin, “Quantum cryptography without bell’s theorem,” *Phys. Rev. Lett.* **68**, 557–559 (1992).
4. C. H. Bennett, D. P. DiVincenzo, J. A. Smolin, and W. K. Wootters, “Mixed-state entanglement and quantum error correction,” *Phys. Rev. A* **54**, 3824–3851 (1996).
5. C. H. Bennett, H. J. Bernstein, S. Popescu, and B. Schumacher, “Concentrating partial entanglement by local operations,” *Phys. Rev. A* **53**, 2046–2052 (1996).
6. D. Deutsch, A. Ekert, R. Jozsa, C. Macchiavello, S. Popescu, and A. Sanpera, “Quantum privacy amplification and the security of quantum cryptography over noisy channels,” *Phys. Rev. Lett.* **77**, 2818–2821 (1996).
7. T. Yamamoto, M. Koashi, and N. Imoto, “Concentration and purification scheme for two partially entangled photon pairs,” *Phys. Rev. A* **64**, 012304 (2001).
8. Z. Zhao, J.-W. Pan, and M. S. Zhan, “Practical scheme for entanglement concentration,” *Phys. Rev. A* **64**, 014301 (2001).
9. J.-W. Pan, C. Simon, c. Brukner, and A. Zeilinger, “Entanglement purification for quantum communication,” *Nature* **410**, 1067–1070 (2001).
10. Z. Zhao, T. Yang, Y.-A. Chen, A.-N. Zhang, and J.-W. Pan, “Experimental realization of entanglement concentration and a quantum repeater,” *Phys. Rev. Lett.* **90**, 207901 (2003).

11. T. Yamamoto, M. Koashi, Ş. K. Özdemir, and N. Imoto, “Experimental extraction of an entangled photon pair from two identically decohered pairs,” *Nature* **421**, 343–346 (2003).
12. D. Stucki, N. Gisin, O. Guinnard, G. Ribordy, and H. Zbinden, “Quantum key distribution over 67 km with a plug&play system,” *New Journal of Physics* **4**, 41 (2002).
13. T. Yamamoto, R. Nagase, J. Shimamura, Ş. K. Özdemir, M. Koashi, and N. Imoto, “Experimental ancilla-assisted qubit transmission against correlated noise using quantum parity checking,” *New Journal of Physics* **9**, 191 (2007).
14. K. Banaszek, A. Dragan, W. Wasilewski, and C. Radzewicz, “Experimental demonstration of entanglement-enhanced classical communication over a quantum channel with correlated noise,” *Phys. Rev. Lett.* **92**, 257901 (2004).
15. A. Laing, V. Scarani, J. G. Rarity, and J. L. O’Brien, “Reference-frame-independent quantum key distribution,” *Phys. Rev. A* **82**, 012304 (2010).
16. J. Wabnig, D. Bitauld, H. Li, A. Laing, J. O’Brien, and A. Niskanen, “Demonstration of free-space reference frame independent quantum key distribution,” *New Journal of Physics* **15**, 073001 (2013).
17. P. Zhang, K. Aungskunsiri, E. Martín-López, J. Wabnig, M. Lobino, W. Nock, R. J. Munns, D. Bonneau, P. Jiang, W. Li, H. A. Laing, G. Rarity, J. O. Niskanen, A. G. Thompson, M. and L. O’Brien, J. “Reference-frame-independent quantum-key-distribution server with a telecom tether for an on-chip client,” *Phys. Rev. Lett.* **112**, 130501 (2014).
18. G. Vallone, V. D’Ambrosio, A. Sponselli, S. Slussarenko, L. Marrucci, F. Sciarrino, and P. Villoresi, “Free-space quantum key distribution by rotation-invariant twisted photons,” *Phys. Rev. Lett.* **113**, 060503 (2014).
19. P. G. Kwiat, A. J. Berglund, J. B. Altepeter, and A. G. White, “Experimental verification of decoherence-free subspaces,” *Science* **290**, 498–501 (2000).
20. M. Bourennane, M. Eibl, S. Gaertner, C. Kurtsiefer, A. Cabello, and H. Weinfurter, “Decoherence-free quantum information processing with four-photon entangled states,” *Phys. Rev. Lett.* **92**, 107901 (2004).
21. T. Yamamoto, K. Hayashi, Ş. K. Özdemir, M. Koashi, and N. Imoto, “Robust photonic entanglement distribution by state-independent encoding onto decoherence-free subspace,” *Nature Photonics* **2**, 488–491 (2008).
22. R. Ikuta, Y. Ono, T. Tashima, T. Yamamoto, M. Koashi, and N. Imoto, “Efficient decoherence-free entanglement distribution over lossy quantum channels,” *Phys. Rev. Lett.* **106**, 110503 (2011).
23. H. Kumagai, T. Yamamoto, M. Koashi, and N. Imoto, “Robustness of quantum communication based on a decoherence-free subspace using a counter-propagating weak coherent light pulse,” *Phys. Rev. A* **87**, 052325 (2013).
24. J. E. Ollerenshaw, D. A. Lidar, and L. E. Kay, “Magnetic resonance realization of decoherence-free quantum computation,” *Phys. Rev. Lett.* **91**, 217904 (2003).
25. L.-A. Wu, P. Zanardi, and D. A. Lidar, “Holonomic quantum computation in decoherence-free subspaces,” *Phys. Rev. Lett.* **95**, 130501 (2005).
26. T. B. Pittman, B. C. Jacobs, and J. D. Franson, “Probabilistic quantum logic operations using polarizing beam splitters,” *Phys. Rev. A* **64**, 062311 (2001).
27. D. F. V. James, P. G. Kwiat, W. J. Munro, and A. G. White, “Measurement of qubits,” *Phys. Rev. A* **64**, 052312 (2001).
28. J. Řeháček, Z. Hradil, E. Knill, and A. I. Lvovsky, “Diluted maximum-likelihood algorithm for quantum tomography,” *Phys. Rev. A* **75**, 042108 (2007).
29. C. K. Hong, Z. Y. Ou, and L. Mandel, “Measurement of subpicosecond time intervals between two photons by interference,” *Phys. Rev. Lett.* **59**, 2044–2046 (1987).

1. Introduction

Faithful distribution of photonic entangled states between two distant parties is one of the significant issues in the field of quantum information processing such as quantum teleportation [1], superdense coding [2] and entanglement-based quantum key distribution [3]. In order to perform these quantum information processing, schemes for robust distribution of entanglement are required. Entanglement distillation [4–6] is one of the protocols for this purpose and several schemes have been proposed and demonstrated experimentally [7–11]. In previous proof-of-principle experiments, photons at visible wavelength were used. However, for practical optical-fiber-based quantum communication over a long distance, photons in telecommunication bands should be used to benefit from a low photon loss in an optical fiber.

In this paper, we report an experimental demonstration of the entanglement extraction based on linear optics and a post-selection [7] by using two non-degenerated photon pairs at a visible wavelength of 780 nm and a telecom wavelength of 1551 nm. The sender Alice keeps the two

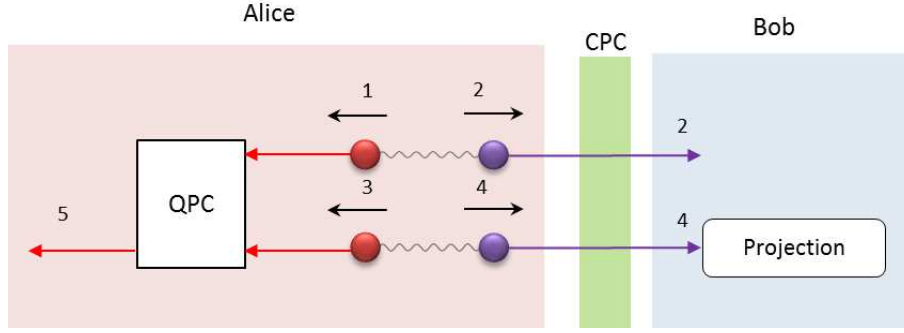


Fig. 1. (Color online) The schematic diagram of the entanglement extraction protocol. Alice generates two polarization entangled photon pairs and sends halves of the photon pairs to Bob through the collective phase-damping channel (CPC). When Alice performs the quantum parity check (QPC) on the two photons in modes 1 and 3, and Bob performs a projection on the photon in mode 4, a maximally entangled photon pair is shared in mode 2 and mode 5.

visible photons and sends the two telecom photons to the receiver Bob through a collective phase damping channel (CPC) which adds the same phase shifts to the two photons. Such a collective noise channel appears in many practical situations [12–14] and discussed in many quantum communication protocols, such as reference-frame-free quantum communication [15–18], decoherence-free quantum communication [19–23] and computation [24, 25]. Through the transmission through the CPC, the entanglement of each photon pair is lost. However, after performing the quantum operation on two photons of 780 nm at Alice’s side and a projective measurement on one of the two photons at Bob’s side, Alice and Bob can extract an entangled photon pair. An observed fidelity of the extracted photon pairs to a maximally entangled state is 0.73 ± 0.07 , which shows extraction of the entanglement from two phase-disturbed photon pairs shared between Alice and Bob.

2. The theory of the entanglement extraction

We first introduce the demonstrated entanglement extraction scheme. The purpose of two parties, Alice and Bob, is to share a maximally entangled photon pair denoted by $|\phi^+\rangle \equiv (|HH\rangle + |VV\rangle)/\sqrt{2}$, where $|H\rangle$ and $|V\rangle$ represent horizontal (H) and vertical (V) polarization states of a photon, respectively. As shown in Fig. 1, Alice generates $\hat{\rho}_{1234} = \hat{\phi}_{12}^+ \otimes \hat{\phi}_{34}^+$, where $\hat{\phi}^+ \equiv |\phi^+\rangle\langle\phi^+|$. The subscripts represent the spatial modes of the photons. She then sends the photons in modes 2 and 4 to Bob through a CPC. By denoting $\hat{Z} \equiv |H\rangle\langle H| - |V\rangle\langle V|$ and $\hat{Z}(\theta) \equiv \exp(-i\theta\hat{Z}/2)$, the CPC acting on the two photons in modes 2 and 4 transforms $\hat{\rho}_{1234}$ to

$$\hat{\rho}'_{1234} = \frac{1}{2\pi} \int d\theta \hat{Z}_2(\theta) \otimes \hat{Z}_4(\theta) \hat{\rho}_{1234} \hat{Z}_2^\dagger(\theta) \otimes \hat{Z}_4^\dagger(\theta) \quad (1)$$

$$= (|HHHH\rangle\langle HHHH| + |HHVV\rangle\langle HHVV| + |HHVV\rangle\langle VVHH| + |VVHH\rangle\langle HHVV| + |VVHH\rangle\langle VVHH| + |VVVV\rangle\langle VVVV|)/4. \quad (2)$$

Because the density operator of each photon pair $\text{Tr}_{34(12)}[\hat{\rho}'_{1234}] = (|HH\rangle_{34(12)}\langle HH|_{34(12)} + |VV\rangle_{34(12)}\langle VV|_{34(12)})/2$ has no entanglement, Alice and Bob do not share any entangled photon pairs as long as they treat the photon pairs separately. However, they can extract a maximally

entangled state of a photon pair from $\hat{\rho}'_{1234}$ of the whole system by local operation and classical communication in the following way.

Alice performs the quantum parity check (QPC) [26] on photons in modes 1 and 3. Kraus operators of the QPC in Fig. 1 is described as $\{\hat{F}, \sqrt{\hat{I} - \hat{F}^\dagger \hat{F}}\}$, where $\hat{F} \equiv |H\rangle_5 \langle HV|_{13} + |V\rangle_5 \langle VH|_{13}$ corresponds to a successful operation of the QPC and the other Kraus operator to a failure operation. After the successful operation of the QPC, the quantum state becomes $\hat{\rho}_{\text{QPC}} \equiv \hat{F} \hat{\rho}'_{1234} \hat{F}^\dagger / \text{Tr} [\hat{F}^\dagger \hat{F} \hat{\rho}'_{1234}] = (|HHV\rangle_{524} \langle HHV|_{524} + |VVH\rangle_{524} \langle HHV|_{524} + |HHV\rangle_{524} \langle VVH|_{524} + |VVH\rangle_{524} \langle VVH|_{524}) / 2$. When Bob performs a projective measurement $\{|+\rangle\langle +|, |-\rangle\langle -|\}$ on the photon in mode 4, where $|\pm\rangle \equiv (|H\rangle \pm |V\rangle) / \sqrt{2}$, the state in modes 2 and 5 is projected onto $|\phi^+\rangle_{25}$ or $|\phi^-\rangle_{25} \equiv (|HH\rangle - |VV\rangle) / \sqrt{2}$. By performing a phase flip operation when the photon in mode 4 is projected onto $|-\rangle$, $|\phi^-\rangle$ is corrected to $|\phi^+\rangle$. As a result, Alice and Bob share $|\phi^+\rangle$ with a success probability $\text{Tr} [\hat{F}^\dagger \hat{F} \hat{\rho}_{\text{QPC}}] = 1/4$. In our experiment, we do not perform the phase flip operation, and the success probability becomes 1/8. We notice that in the scheme, the effect of the phase disturbance on the photons in modes 2 and 4 is compensated by the QPC on the photons 1 and 3 at Alice's side. Such a non-local cancellation of the phase fluctuation is the result of the use of a significant property of the maximally entangled states, which is described by the relation $(\hat{I}_{1(3)} \otimes \hat{Z}_{2(4)}) |\phi^+\rangle_{12(34)} = (\hat{Z}_{1(3)} \otimes \hat{I}_{2(4)}) |\phi^+\rangle_{12(34)}$ [22, 23].

3. Experiment

3.1. Experimental setup

The experimental setup is shown in Fig. 2 (a). Two entangled photon pairs are generated by spontaneous parametric down conversion (SPDC) at source A and B. The setup of the photon pair sources is shown in Fig. 2 (b). The pump laser is based on a fiber laser (wavelength: 1037 nm, pulse width: 381 fs, repetition rate: 80 MHz), which is frequency doubled such that the center wavelength is 519 nm with the power of 1.32 W. The polarization of the pump beam is set to be diagonal to the axes of two adjacent phase-matched 1-mm-thick β -barium borate (BBO) crystals by the half wave plate (R45). In this experiment, we select the non-degenerate photon pair at a visible wavelength of 780 nm and a telecom wavelength of 1551 nm among the photon pairs generated from the BBOs. After the BBO crystal, the pump beam is removed by using a pair of dichroic mirrors (DM1) whose reflectance for the photons at 780 nm and 1551 nm is over 99 % and transmittance for the photons at 519 nm is ~ 97 %. After DM1, the visible photons and telecom photons are separated into different spatial modes by DM2. For both photons, the group delays between $|H\rangle$ and $|V\rangle$ are compensated by 6.17 mm and 7.44 mm-thick quartz crystals (Quartz1) in the paths of the visible and the telecom photons, respectively. The relative phase shift between $|HH\rangle$ and $|VV\rangle$ is compensated by tilting 0.6 mm-thick quartz crystals (Quartz2).

As shown in Fig. 2 (a), two visible photons from photon source A and B are injected into a polarizing beamsplitter (PBS) simultaneously by adjusting a moving mirror (M). The spectra of the two output photons from the PBS are filtered by interference filters (IFs) with a bandwidth of 3 nm, and then coupled to single-mode fibers followed by silicon avalanche photodetectors (quantum efficiency: 60 %) D1 and D3. On the other hand, two telecom photons pass through a liquid crystal retarder (LCR). The LCR adds eight phase shifts $n\pi/4$ ($n = 0, 1, 2, \dots, 7$) between $|H\rangle$ and $|V\rangle$ of the two photons by switching the applied voltage. The operations of the LCR on the two photons are nominally described by the Kraus operators $\{\hat{Z}_2^{n\pi/4} \otimes \hat{Z}_4^{n\pi/4}\}_{n=0,1,2,\dots,7}$. Because this transformation is exactly the same completely positive and trace preserving map as the one given in Eq. (1), the LCR simulates the CPC. The telecom photons are sent through the interference filters (IFs) with a bandwidth of 10 nm and then they are coupled to single-mode fibers followed by two InGaAs avalanche photodetectors (quantum

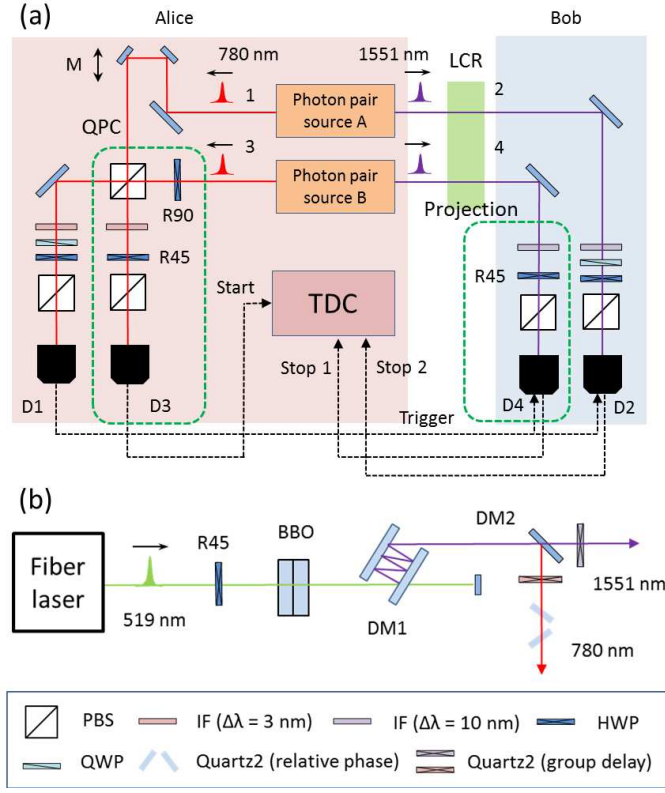


Fig. 2. (Color online) (a) The experimental setup for the entanglement extraction. The half wave plate R90 transforms $|H\rangle$ to $|V\rangle$ and vice versa. The half wave plate R45 transforms $|H\rangle$ to $|+\rangle$ and $|V\rangle$ to $|-\rangle$, and vice versa. (b) The experimental setup of photon sources A or B. The pulsed pump light (519 nm) is obtained by frequency doubling the output light of the mode locked fiber laser at 1037 nm. The details are shown in the main text.

efficiency: 25 %) D2 and D4 which are gated by the electric signal from D1. The electric signal from D3 is connected to a time-to-digital converter (TDC) as a start signal, and electric signals from D2 and D4 are used as stop signals of the TDC. We postselect the events where two stop signals are clicked within the time difference of 2 ns, which guarantees the four-fold coincidence among D1, D2, D3 and D4.

3.2. Experimental results

We first characterized the initial two photon pairs from photon pair sources A ($\hat{\rho}_{12}$) and B ($\hat{\rho}_{34}$). By performing the quantum state tomography [27] with diluted maximum-likelihood algorithm [28], we reconstructed the density operators of the photon pairs as shown in Figs. 3 (a) and (b). Observed fidelities of $\hat{\rho}_{12}$ and $\hat{\rho}_{34}$ to $|\phi^+\rangle$ were 0.92 ± 0.01 and 0.94 ± 0.01 , respectively, which implies that the two photon pairs were highly entangled. The detection rates of $\hat{\rho}_{12}$ and $\hat{\rho}_{34}$ were 920 Hz and 620 Hz, respectively. We estimated that the photon pair generation rate is of the order of 10^{-2} , which indicates that the multi-photon emission from the photon sources is negligibly small.

Next we reconstructed the density operators when we applied phase fluctuations to each pho-

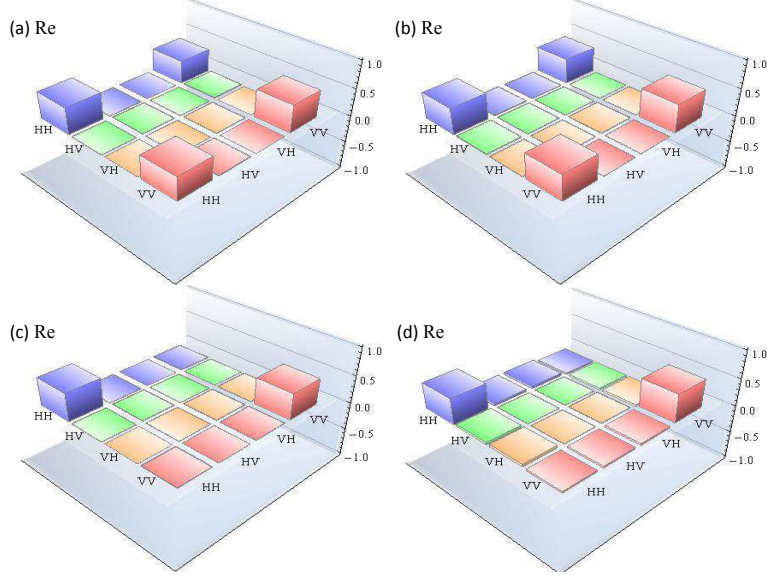


Fig. 3. (Color online) The real parts of the matrix elements of (a) $\hat{\rho}_{12}$, (b) $\hat{\rho}_{34}$, (c) $\hat{\rho}'_{12}$ and (d) $\hat{\rho}'_{34}$.

ton pair by using the LCR. Figures. 3 (c) and (d) show the reconstructed density matrices of $\hat{\rho}'_{12}$ and $\hat{\rho}'_{34}$ with phase fluctuations. Off-diagonal elements of the density matrices disappeared, which indicates that the LCR effectively simulates the phase-damping channel. Observed fidelities of $\hat{\rho}_{12}$ and $\hat{\rho}_{34}$ to $|\phi^+\rangle$ were 0.50 ± 0.01 and 0.46 ± 0.02 , respectively.

Before demonstrating the entanglement extraction scheme, we performed the Hong-Ou-Mandel (HOM) interference [29] of the photons in modes 1 and 3 which are heralded by the photon detection at D4 and D2, respectively. The experimental result is shown in Fig. 4. We clearly observed the HOM dip around zero delay point. The observed visibility at zero delay was 0.80 ± 0.05 . The full width at the half maximum (FWHM) was calculated as $\sim 204 \mu\text{m}$ by fitting the experimental data with the Gaussian.

Finally, we reconstructed the density operator $\hat{\rho}_{\text{final}}$ when we performed the entanglement extraction scheme on the two photon pairs. The experiment was performed at the zero delay point of the HOM dip in Fig. 4. The reconstructed density matrix is shown in Fig. 5. An observed fidelity of $\hat{\rho}_{\text{final}}$ to $|\phi^+\rangle$ was 0.73 ± 0.07 , clearly exceeding the threshold value of 0.5 to show that the extracted pair of photons are entangled. This means that entanglement was successfully distributed at the telecom regime in the presence of corrective phase fluctuations.

4. Discussion

In the following, we consider the reason for the degradation of the observed values of the visibility of the HOM interference between the photons in modes 1 and 3 and the fidelity of $\hat{\rho}_{\text{final}}$ after the entanglement extraction scheme. Because the probability of the multi-photon pair emission is sufficiently low, the two-photon state obtained by SPDC after IFs is expressed as

$$|\Psi\rangle_{ij} \simeq \iint d\omega d\omega' \Phi(\omega, \omega') \hat{a}_i^\dagger(\omega) \hat{a}_j^\dagger(\omega') |\text{vac}\rangle, \quad (3)$$

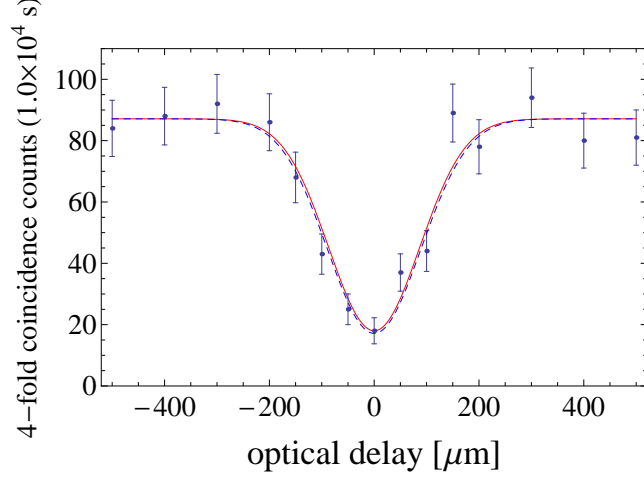


Fig. 4. (Color online) The observed Hong-Ou-Mandel interference between two visible photons in modes 1 and 3. Each point was recorded for 1.0×10^4 s. The red solid curve is the Gaussian fit to the obtained data. The blue dashed curve is obtained by Eq. (4) with experimental parameters.

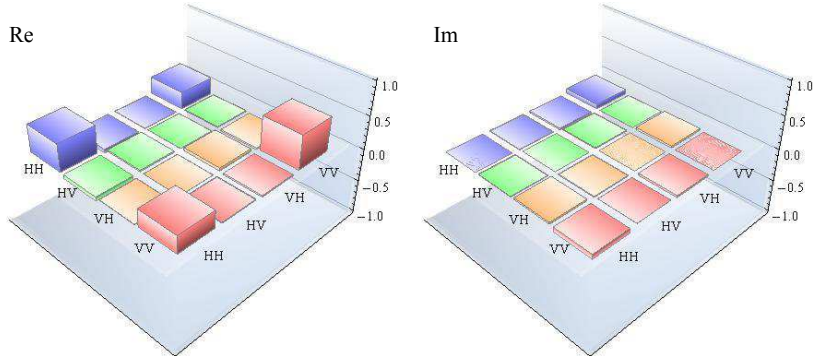


Fig. 5. (Color online) (left) the real part and (right) imaginary part of the density operator $\hat{\rho}_{\text{final}}$ of the extracted photon pair.

where $|\text{vac}\rangle$ is the vacuum state, and $\hat{a}_k^\dagger(\omega)$ is a creation operator at the angular frequency of ω in spatial mode $k(=1,2,3,4)$. $\Phi(\omega, \omega')$ is a product of the spectral amplitude of the two-photon state generated from the SPDC and the transmission coefficients of the IFs for the visible and telecom photons. Because the detectors distinguish neither angular frequencies nor exact arriving times of the photons, the four-fold coincidence probability P_{1234} among the detectors D1, D2, D3 and D4 is given by the sum of all the frequency contributions, which is proportional to $\iiint d\omega_1 d\omega_2 d\omega_3 d\omega_4 |\langle \text{vac} | \hat{a}_1(\omega_1) \hat{a}_3(\omega_3) \hat{U} | \phi(\omega_2) \rangle_1 \langle \phi(\omega_4) \rangle_3|^2$. Here $|\phi(\omega_2)\rangle_1 \equiv \langle \text{vac} | \hat{a}_2(\omega_2) | \Psi \rangle_{12} = \int d\omega \Phi(\omega, \omega_2) \hat{a}_1^\dagger(\omega) | \text{vac} \rangle$ and $|\phi(\omega_4)\rangle_3 \equiv \langle \text{vac} | \hat{a}_4(\omega_4) | \Psi \rangle_{34} = \int d\omega \Phi(\omega, \omega_4) \hat{a}_3^\dagger(\omega) e^{i\omega\tau} | \text{vac} \rangle$, where τ is the time delay in mode 3. The unitary operator \hat{U} represents the transformation at the HBS, which satisfies $\hat{U} | \text{vac} \rangle = | \text{vac} \rangle$, $\hat{U} \hat{a}_1^\dagger(\omega) \hat{U}^\dagger = (\hat{a}_1^\dagger(\omega) + \hat{a}_3^\dagger(\omega)) / \sqrt{2}$ and $\hat{U} \hat{a}_3^\dagger(\omega) \hat{U}^\dagger = (\hat{a}_1^\dagger(\omega) - \hat{a}_3^\dagger(\omega)) / \sqrt{2}$. In our experiment, we assume that phase matching bandwidth of the BBO crystal is sufficiently broad, and the spectral

distribution function of the pump beam for the photon pairs is a Gaussian with a variance $\delta\omega_p$ and a center angular frequency ω_p , and those of the IFs for the visible/telecom photons are Gaussians with a variance $\delta\omega_{v/t}$ and a center angular frequency $\omega_{v/t}$. By these assumptions, $\Phi(\omega, \omega')$ is represented as $\Phi(\omega, \omega') = \exp[-(\omega + \omega' - \omega_p)^2 / (4\delta\omega_p^2)] \exp[-(\omega - \omega_v)^2 / (4\delta\omega_v^2)] \exp[-(\omega' - \omega_t)^2 / (4\delta\omega_t^2)]$. Then P_{1234} is calculated as

$$P_{1234} \propto 1 - \sqrt{\frac{\delta\omega_p^2(\delta\omega_p^2 + \delta\omega_v^2 + \delta\omega_t^2)}{(\delta\omega_v^2 + \delta\omega_p^2)(\delta\omega_t^2 + \delta\omega_p^2)}} e^{-\frac{\delta\omega_v^2 \delta\omega_p^2 \tau^2}{\delta\omega_v^2 + \delta\omega_p^2}}. \quad (4)$$

The coefficient of the second term in right hand side of Eq. (4) is the visibility of the HOM dip. In our experiment, we use the pump beam at 519 nm with a pulse width of 397 fs, the interference filters with a bandwidth of 3 nm for the visible photons at 780 nm and those with a bandwidth of 10 nm for the telecom photons at 1551 nm. These values correspond to $\delta\omega_p \simeq 3.0 \times 10^{12} \text{ s}^{-1}$, $\delta\omega_v \simeq 3.9 \times 10^{12} \text{ s}^{-1}$ and $\delta\omega_t \simeq 3.3 \times 10^{12} \text{ s}^{-1}$. The dependency of the visibility on τ is predicted as in Fig. 4. The visibility at zero delay and the FWHM of the dip are found to be 0.80 and 210 μm . We see that the theoretical curve is in good agreement with the experimental results. Thus we expect that a higher visibility will be obtained by using a narrower spectral filtering.

Next, we consider the reason for the degradation of the fidelity of $\hat{\rho}_{\text{final}}$ after the entanglement extraction scheme. We assume that the visibility of the HOM interference does not depend on the polarization of the photons. We also assume that each input pulse is described by a photon in a single temporal and spatial mode, and the overlap (indistinguishability) between the two mode shapes is given by the observed visibility of 0.80. By using the reconstructed density operators of $\hat{\rho}_{12}$ and $\hat{\rho}_{34}$ in Figs. 3 (a) and (b) as the initial photon pairs, the fidelity of the two-photon state after the entanglement extraction is calculated to be 0.79, which is within the margin of the statistical error of our experimental result. In this model, the degradation of the fidelity is caused by the imperfection of the initial state and the visibility of the HOM interference. If we prepare the maximally entangled states $\hat{\phi}_{12}^+$ and $\hat{\phi}_{34}^+$ as the initial photon pairs and the visibility of HOM interference is 0.80, the fidelity of the extracted state is calculated to be 0.90. If we use the narrower IFs such that the visibility is 1, the fidelity of the final two-photon state is calculated to be 0.87 from the initial states $\hat{\rho}_{12}$ and $\hat{\rho}_{34}$.

5. Conclusion

In conclusion, we have demonstrated the entanglement extraction scheme using the polarization entangled photon pairs at the visible wavelength of 780 nm and the telecom wavelength of 1551 nm. The observed fidelity of the extracted photon pair is 0.73 ± 0.07 , which clearly shows the recovery of the entanglement shared between the parties. While this scheme was demonstrated for distributing entangled photon pairs against collective phase noise, it is also applicable to the entanglement distribution against general collective noises for two qubits by sending H-polarized and V-polarized photons through different channels as proposed in Ref. [13]. We believe that our result is useful for the efficient and robust distribution of entanglement through optical fibers over a long distance.

Acknowledgments

This work was supported by the Funding Program for World-Leading Innovative R&D on Science and Technology (FIRST), MEXT Grant-in-Aid for Scientific Research on Innovative Areas 21102008, JSPS Grant-in-Aid for Scientific Research(A) 25247068, (B) 25286077 and (B) 26286068.